Journal of Information Systems Engineering and Management
2025, 10(14s)
e-ISSN: 2468-4376
https://www.jisem-journal.com/

Research Article

Rutting Evaluation of Hot Mix Asphalt Using Finite Element Modeling Based on Viscoplastic Characteristics from Static Creep Test

Ali A. Kamal [1,2, a,] Hasan Al-Mosawe [2]

[1]*Environment and Pollution Engineering Techniques Department, Technical Engineering College - Kirkuk, Northern Technical University, Iraq*

[2] *Civil Engineering, Al-Nahrain University, Baghdad, Iraq*

[a)] *Corresponding author: ali.engi1992@ntu.edu.iq*

ARTICLE INFO

Received: 19 Nov 2024

Revised: 10 Jan 2025

Accepted: 24 Jan 2025

ABSTRACT

among the foremost widespread road damages is rutting in asphalt surfaces, which can be prevented or lessened with the Bailey technique. In order to estimate rut depth in hot mix asphalt (HMA) blends, this article simulates wheel track testing using the two-dimensional (2D) as well as three-dimensional (3D) finite-element method (FEM). It then connects these characteristics with an accelerated performance testing tool. In order to simulate the viscoplastic properties of bituminous mixes, static creep experiments are conducted on several samples to determine the substance parameters of the creep power law. The Hamburg wheel rut tester (HWRT) can be utilized to calibrate material characteristics produced in a static creep test and rut asphalt laboratory-accelerated rutting resistance analysis. HWRT is simulated using finite-element programs, and results from the model have been compared with the results of the experiment. According to the findings, there is a range of 0.2 to 6.6% between the predicted and actual rut depths in the laboratory's measurements.

Keywords: Rutting Evaluation, Hot Mix Asphalt, Finite Element Modeling, Viscoplastic Characteristics, Wheel Tracking Test, Static Creep Test.

INTRODUCTION

Rutting, particularly in hot mix asphalt (HMA) pavement, is one of the critical distresses that can be seen on the surface of flexible pavements. Due to frequent strong traffic volumes, permanent deformation can happen through a variety of mechanisms, including densification, shear deformation, and/or material loss under the wheel path (Ali et al., 2017). Over time, the repeated stress that traffic volume imposes on flexible pavements eventually develops rutting or permanent deformation. The operation of rutting beginning and progressing in flexible pavements is influenced by a growing percentage of loading conditions. Rutting occurs at various intervals throughout the period of serviceability of flexible pavements. Generally speaking, rutting can be categorized into two basic types. The first type occurs after some years of construction of the flexible pavement due to densification (rise in density and reduction in volume) and is known as initial rutting, whereas the second type is called secondary rutting, also known as shear deformation, which results from movement of asphalt materials just below the wheel path that causes upheaval on both sides of tires (Irfan et al., 2018).

HMA is a composite material made up of air spaces, various-sized aggregate fragments, and an asphalt binder containing or not containing additives. The characteristics of the various ingredients and their relative proportions determine how HMA reacts to traffic volumes and climatic circumstances. The response of the mixture to loads, in turn, is significantly associated with the performance of HMA in terms of rutting, cracking, and durability (Vavrik et al., 2002). Several investigations suggest that the asphalt layers are the primary location for pavement rutting and that the design of asphalt mixes and the suitability of the components possess a major impact on this problem (Aodah, 2013). Thus, the primary topic of the present dissertation is the rutting performance of asphalt blends, which is going to be covered in greater detail in the subsequent sections.

With the goal to generate a rut-resistant blend of asphalt while preserving the appropriate durability behaviors, the aggregate structure in the Superpave mix design is built utilizing the Bailey approach, since the aggregate gradation represents one of the primary variables that directly influences rutting.

The Finite Element Method (FEM) is a strong computational and numerical method for resolving intricate mathematics and engineering issues. The finite element method is especially useful in fluid dynamics, heat transport, structural analysis, and other fields. The FEM's fundamental concept is to split a complicated

domain into simple subdomains, such as triangles and quadrilaterals, known as finite elements (Bathe, 1996; Cook et. al., 2002). Each of these elements is connected to one another by common nodes (Holanda et al., 2006; Carvalho, 2012). This approach's most alluring feature is its capacity to resolve extremely challenging engineering issues, particularly when computer software is included. To solve the large matrices that are produced during the analysis using this method, computer software is necessary. ABAQUS, a publicly available finite element program frequently used in pavement engineering research, was used to execute the visco-plastic model created and calibrated in the current investigation. The goal was to develop a reliable and user-friendly tool for predicting the rutting of hot asphalt mixtures. For this kind of application, ABAQUS is a useful tool for a number of considerations. This finite element analysis program is well-established, validated, and documented. After the study is finished, it is easier to create models and visualize the results due to its user-friendly pre- and post-processing interface. Its library also includes many multiple types of elements which capable of modeling any configuration, and there are many different materials' behavioral models that are capable of modeling the behaviour of various materials employed in engineering (ABAQUS, 2014; Bakhshi and Arabani, 2018). Additionally, ABAQUS is a collection of robust engineering simulation tools that can tackle a variety of engineering issues, from the most difficult nonlinear simulations to comparatively easy linear assessments (Ebrahimi, 2015).

The aim of this research paper is to investigate the static creep test in order to find a model that accurately represents the rutting (permanent deformation) of hot mix asphalt of various aggregate grades prepared using the Bailey technique.

TECHNIQUES AND STUDY STRATEGY

Within the present investigation, a 2D and 3D finite element modeling program was used to forecast the rut depth of the hot mix asphalt. The findings have been evaluated to the actual rut depths obtained from the wheel tracking test. The ABAQUS software's time-hardening creep power law model was utilized to simulate the asphalt surface as a viscoplastic material. Bituminous specimens had been subjected to static creep tests in order to determine the creep power law's parameters. For the static creep test, the stress values of 10, 20, and 30 psi at 25, 40, and 55 °C were chosen. The necessary creep power law model parameters were obtained by data graph computation. The initial creep settings were then calibrated using the results of wheel track testing. Finally, these models were validated by comparing the calibrated rut depths of the 2D and 3D FEM with experimental results.

MATERIALS AND DESIGN METHOD OF HOT MIX ASPHALT

This part presents the materials that were chosen and prepared, including each material's physical characteristics. The materials preparation stage comprises crushed gravel, crushed sand, river sand, filler, and neat asphalt binder. The following parts cover the Hot Asphalt Mixtures used, the procedure to prepare a Superpave specimen includes figuring out the binder's viscosity, picking an appropriate performance grade, deciding on the mixing and compaction temperatures, developing aggregate gradation using the Bailey approach, and figuring out the optimum binder mix percentage for dense graded mixtures. The last section is the experimental procedure covering binder morphological characterization and mixture performance tests.

1.1 Materials Selection and Preparation

The materials that were employed in the present research are frequently utilized in asphalt construction projects in Iraq's central and southern areas and are readily available locally. Along with mineral filler (cement), they also incorporate neat binders of asphalt and mineral aggregates. The following paragraphs assess the qualities of these materials while comparing the results to the specifications of Superpave and the specification limits of the State Corporation for Roads and Bridges in Iraq (SCRB/R9, 2003).

1.1.1 Mineral Aggregates

Crushed gravel, crushed sand, and river sand have been selected as the three aggregate types that are most often used in Iraq for the surface course of flexible pavements. **Table (1)** displays the physical characteristics of the crushed gravel, crushed sand, and river sand employed in the current research. To ensure that the chosen aggregates are suitable for the Hot Mix Asphalt design, experimental Superpave evaluations were carried out and assessed alongside the required specifications as described in **Table (2)**. The gradation of the selected types of aggregate is illustrated in **Table (3)**.

Table (1) Physical characteristics of the crushed gravel, crushed sand, and river sand.

Measured properties	ASTM/AASHTO Designation	Test Results		
		Coarse Aggregate	Fine Aggregate	
		Crushed Gravel (CG)	Crushed Sand (CS)	River Sand (RS)
Bulk Specific Gravity	ASTM C127-15 AASHTO T 85-14 & ASTM C128-15 AASHTO T 84-13	2.598	2.637	2.625
Apparent Specific Gravity		2.657	2.702	2.691
Water Absorption, %		0.631	1.401	0.862

Table (2) Superpave tests results of the crushed gravel, crushed sand, and river sand.

Measured Properties / Consensus Properties	Superpave Requirements	Test Results		
Coarse Aggregate Angularity (CAA), %	Min. 95/90	98 %		
Fine Aggregate Angularity (FAA), %	Min. 45	52 %		
Flat and Elongated particles (F&E), %	Max. 10	2 %		
Sand Equivalent (SE), %	Min. 45	61 %		
Source Properties	**Superpave Requirements**	**Test Results**		
		Coarse Aggregate	Fine Aggregate	
			Crushed sand	River sand
Toughness by Los Angeles abrasion, %	Max. 30	18.68 %	-	-
Soundness test by Na_2SO_4, %	Max. 15	2.86 %	1.14 %	1.21 %
Deleterious materials %	0.2 - 10	0.31 %	3.3 %	3.5%

Table (3) Aggregate gradation results for the crushed gravel, crushed sand, and river sand.

Sieve Size		Coarse Aggregate	Fine Aggregate	
inch	mm	Crushed Gravel	Crushed Sand	River Sand
3/4"	19	100	100	100
1/2"	12.5	89.7	100	100
3/8"	9.5	58.2	100	100
No.4	4.75	29.6	97.6	96.2
No.8	2.36	5.1	82.6	80.2
No.16	1.18	3.6	50.1	65.7
No.30	0.6	0.1	23.2	45.4
No.50	0.3	0.1	17.2	12.9
No.100	0.15	0	6.4	4.6
No.200	0.075	0	2.1	1.8

2.1.2. Filler Material

Ordinary Portland Cement from Kufa Cement Plant in Al-Najaf Province - Kufa District - Al-Barakiyah was used as filler material for the preparation of the Hot Mix Asphalt samples in the current study. **Table (4)** summarize the physical characteristics of the filler that was employed. As stated in ASTM C110-16, the following tests are performed.

Table (4): Ordinary Portland Cement physical characteristics.

Property	SCRB specification	Test Result
Specific Gravity (G_{filler})	/	3.12
% passing sieve No.200 (0.075 mm)	70 - 100	100

2.1.3. Neat Binder

The binder utilized in the current research was the asphalt binder that is manufactured in the AL-Daurah Refinery with a penetration grade of (40-50). The characteristics of the asphalt binder were summarized in **Table (5)**. While the Superpave performance-graded (PG) of Asphalt Binder demonstrated in **Table (6)**.

Table (5): Physical characteristics of Neat Binder.

Binder Tests	ASTM Designation	Test results	SCRB Requirements
Penetration (25 °C, 100 g, 5 s, 0.1 mm)	D 5	42	40 – 50
Flashpoint (Cleveland open cup)	D 92	262	> 230 °C
Softening point (Ring & Ball)	D36	53.9	50 °C – 58 °C
Ductility (25 °C)	D 113	+100	> 100 cm
Specific gravity @ 25 °C	D 70	1.04	(1.01 – 1.06) gm/cm^3
Solubility in C_2HCL_3, %Wt	D 2042	99.9	> 99.0
Absolute viscosity at 60 °C	D 2171	4152.6	(4000 ± 800) Poise
Kinematics viscosity at 135 °C	D 2170	628.1	> 400 cSt
%Wt Loss in Heating (50g, 5h @ 163°C)	D 1754	0.028	< 0.5
% Original of Penetration after loss in heat (25 °C, 100 g, 5 s, 0.1 mm)	D1754 & D5	91	> 75
Ductility of residue (25 °C)	D1754 & D113	64	> 25

Table (6): Rheological characteristics of Asphalt Binder (40-50).

Aging Condition: Original binder (Un-aged)			
Type of Test	**Temperature**	**Test Results**	**AASHTO T-315 Requirements**
Rotational Viscometer (RV) **Viscosity**	135 C°	0.523	≤ 3 Pa.s
	165 C°	0.138	
Dynamic Shear Rheometer (DSR) **| G* | / Sin δ** @ 10 rad/s, Kpa.	58 C°	4.476	≥ 1 KPa
	64 C°	1.859	
	70 C°	0.858	
Aging Condition: RTFO Residue (Short-term aging)			
Type of Test	**Temperature**	**Test Results**	**AASHTO T-315 Requirements**
Dynamic Shear Rheometer (DSR) **| G* | / Sin δ** @ 10 rad/s, Kpa.	58 C°	5.918	≥ 2.2 KPa
	64 C°	3.352	
	70 C°	1.886	
Aging Condition: PAV Residue (Long-term aging)			
Type of Test	**Temperature**	**Test Results**	**AASHTO T-315 Requirements**
Dynamic Shear Rheometer (DSR) **| G* | / Sin δ** @ 10 rad/s, Kpa.	22 C°	9878	≤ 5000 KPa
	25 C°	8641	
	28 C°	4372	
Bending Beam Rheometer (BBR) **Creep Stiffness (S)** @ 60 sec.	0 C°	72.35	≤ 300 MPa
	-6 C°	148.71	
	-12 C°	378.47	
Bending Beam Rheometer (BBR) **m-value** @ 60 sec.	0 C°	0.376	≥ 0.3
	-6 C°	0.311	
	-12 C°	0.262	

2.2. SUPERPAVE Mixtures Design

Superpave is a technique for creating asphalt mixtures that entail a series of four crucial steps: choosing the appropriate material, designing the aggregate structure (DAS), determining the design asphalt content (DAC), as well as assessing the moisture sensitivity of mixtures.

2.2.1. Bailey Approach for Designing the Aggregate Structure (DAS)

The major goal of this research project is to create the aggregate structure utilizing an analytical aggregate gradation method that will enable a sensible merging of various aggregate sizes to produce a densely packed

aggregate skeleton for excellent stability and appropriate VMA. For this, the Bailey technique to perform a gradation assessment of the aggregate has been used.

The equivalent unit weight for each kind of aggregate as well as the size of the sieve distribution must be obtained for the Bailey technique, which is frequently employed in dense-graded mix designs. The Bailey approach determines the Loose Unit Weight (LUW) and Rodded Unit Weight (RUW) for coarse aggregate and the RUW for fine aggregate following the procedures established by AASHTO T19-14.

The aggregate structure is designed by Bailey's approach calculations. For example, in a mixture of (CACUW%) equal to (65%), the Bailey Approach procedure would be as in the following **Table (7)**:

Table (7): Results from the Bailey Approach procedure for the blend of (65%) Coarse Aggregate Chosen Unit Weight.

Sieve Size		**Coarse Aggregate Blend by Volume**	**Fine Aggregate Blend by Volume**		**% Passing Sieve No.200**	**Obtained Gradation**
inch	**mm**	**CG**	**CS**	**RS**	**MF**	
		100%	**75%**	**25%**		
3/4"	19	100	100	100	100	100.00
1/2"	12.5	89.7	100	100	100	96.15
3/8"	9.5	58.2	100	100	100	84.38
No.4	4.75	29.6	97.6	96.2	100	72.08
No.8	2.36	5.1	82.6	80.2	100	54.09
No.16	1.18	3.6	50.1	65.7	100	37.44
No.30	0.6	0.1	23.2	45.4	100	21.56
No.50	0.3	0.1	17.2	12.9	100	14.08
No.100	0.15	0	6.4	4.6	100	8.17
No.200	0.075	0	2.1	1.8	100	5.91
CUW of Coarse Aggregates %		65 %				
RUW of Fine Aggregates %			100 %			
LUW (kg/m3)		1382.4				
RUW (kg/m3)		1557.1	1653.6	1754.2		
Chosen Unit Weight (CUW)		898.56	1653.6	1754.2		
Bulk Specific Gravity, G_{sb}		2.598	2.637	2.625		
Percentage of Voids between CA		65.4%				
Unit Weight contributed by each Aggregate		898.560	811.257	286.870		
Unit Weight of Blend (UWB)		1996.687				
Initial Blend Percentage		45.0%	40.6%	14.4%		
% Fine aggregate in the coarse stockpile to its portion in a mix		2.295%				
% Coarse aggregate in the fine stockpile to its portion in a mix			7.064%	2.851%		
Justified blend percentage		37.38%	46.32%	16.3%		
% Passing Sieve No.200		0.00%	0.97%	0.29%		
Desired Mineral Filler %					6.00%	
Needed Mineral Filler %					4.74%	
Proportions of the Final Mixture		**37.38%**	**42.77%**	**15.11%**	**4.74%**	

Table (8) illustrates the Bailey Ratios (Aggregate Ratios) of 12.5 mm NMAS for the selected four types of hot asphalt mixtures with specification limits of Superpave. Subsequent to this, Figure **(1)** shows the gradation of designated aggregate blends for the present research.

Table (8): Bailey Ratios (Aggregate Ratios) of 12.5 mm NMAS for four types of hot asphalt mixtures with specification limits of Superpave.

Aggregate Mixtures	Bailey Ratios (Aggregate Ratios) for 12.5 mm NMAS					
	Coarse Graded Mixture			Fine Graded Mixture		
	CA%	FA_c%	FA_f%	New CA%	New FA_c%	New FA_f%
MX 1 (65% CACUW)	0.64	0.398	0.378	0.97	0.378	The size of the sieves was too small to estimate the value.
MX 2 (85% CACUW)	0.52	0.408	0.427	1.0	0.427	
MX 3 (96% CACUW)	0.50	0.415	0.461	/	/	
MX 4 (104% CACUW)	0.45	0.421	0.490	/	/	
Recommended Ratios	0.5-0.65	0.35-0.5	0.35-0.5	0.6-1.0	0.35-0.5	0.35-0.5

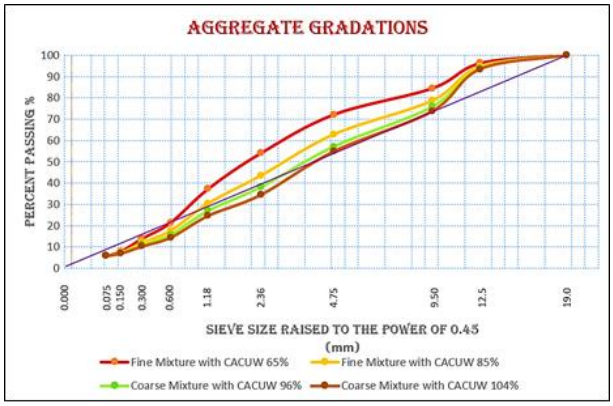

Figure (1): Gradation of designated aggregate blends.

2.2.3. Mixing and compaction temperatures of asphalt mixtures

The viscosity of unmodified bitumen is typically measured using a rotational Brookfield viscometer utilizing the conventional standard method (D4402) / (AASHTO T 316) at temperatures of (135 C°) as well as (165 C°) with the objective of selecting the mixing and compaction temperatures of hot mixes asphalt. When using the equiviscous approach, the asphalt's temperature shall be raised to achieve viscosity values associated with (0.17 ± 0.02 Pa.s) followed by (0.28 ± 0.03 Pa.s), which will be used to decide the temperatures for mixing and compacting of hot asphalt mixtures, as demonstrated in **Figure (2)**.

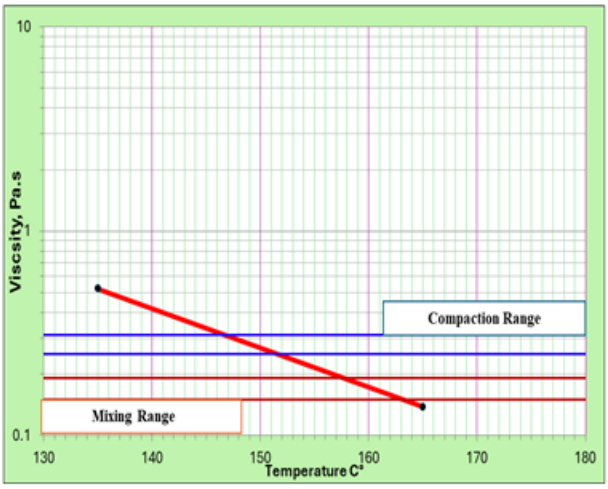

Figure (2): Mixing and compaction temperatures of asphalt mixtures.

According to the generated plot, the compaction as well as mixing temperatures for the neat bitumen utilized in the present research are 149 and 160.5 Celsius degrees, in that order.

2.2.4. Determination of Trial (Initial) Binder Content for Trial Blends

In accordance with the typical bitumen amounts for the designed aggregate structure recommended by the Asphalt Institute, the initial bitumen value was chosen as 5 percent. The objective was to determine the percentage of bitumen needed for the compacted specimens in order to satisfy the 4% designed air void content. According to the findings from compacted testing samples, an estimated design amount of bitumen will be determined (Institute, 2014). The estimated percentage of asphalt for each type of mixture is presented in **Table (9)**.

Table (9): Estimated Bitumen amounts for the chosen aggregate blends.

Mixture Kind	MX 1 (65% CACUW)	MX 2 (85% CACUW)	MX 3 (96% CACUW)	MX 4 (104% CACUW)
$P_{b\ estimated}$ %	5.5	5.0	4.9	4.8

2.2.5. Choosing Optimum Bitumen Content

For obtaining the optimum bitumen content or the design asphalt content (DAC), three samples corresponding to each chosen blend have been generated and compacted using the following four bitumen amounts:

- Pb estimated %.
- Pb estimated % + 0.5 %.
- Pb estimated % - 0.5 %.
- Pb estimated % + 1.0 %.

The Optimum Bitumen Content will be selected as the amount that satisfies the (4%) air void proportion after which the remaining volumetric parameters at (Nini) and (Nmax) are determined and checked in accordance with the recommended requirements. **Figure (3)** presented the volumetric properties against the bitumen percentage of the designed blend within (65% CACUW). **Table (10)** presents the design characteristics for selected mixtures with (12.5 mm NMAS).

Table (10): Summary of the mix design properties for the chosen aggregate blends.

Mix Properties	Designed Mixtures			
	MX1 65% CACUW	MX2 85% CACUW	MX3 96% CACUW	MX4 104% CACUW
Va% @N_{des}	4 %	4 %	4 %	4 %
	Requirements (4%)			
OAC %	5.6	5.2	5.1	5.3
	Requirements (4% - 6%)			
G_{mm}% @N_{ini}	87.45	87.73	87.24	87.17
	Requirements (≤ 89%)			
VMA %	15.83	15.28	15.05	14.85
	Requirements (≥ 14%)			
VFA %	74.7	73.8	73.4	73
	Requirements (65% - 75%)			
DP	1.07	1.16	1.18	1.14
	Requirements (0.6% - 1.2%)		Requirements (0.8% - 1.6%)	
G_{mm}% @N_{max}	96.63	97.34	97.02	97.45
	Requirements (≤ 98%)			

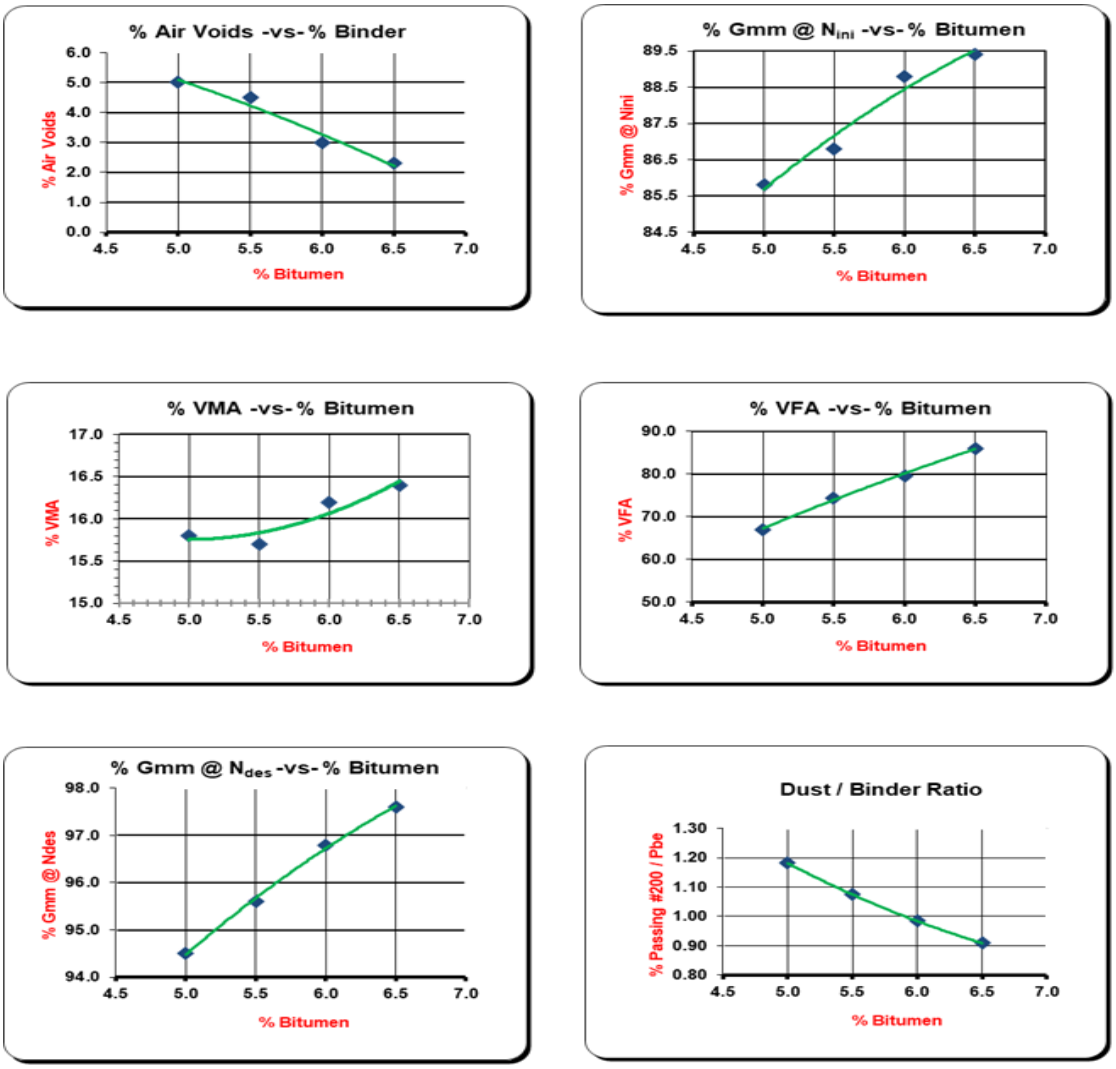

Figure (3): volumetric properties against the bitumen percentage of the designed blend within (65% CACUW).

2.2.6. Moisture Susceptibility Testing

Moisture susceptibility testing is the final stage in the Superpave mix design procedure. The moisture susceptibility of a mixture is assessed by examining it dry and then soaking it for specific periods of time. The Lottman Test (ASTM D 4867) serves as a typical approach to evaluating moisture susceptibility and stripping. For this test, six specimens are compacted to (7 ± 1 %) air voids.

The Summary of the moisture susceptibility data for each type of bitumen mixture is presented in **Table (11)**. The typical tensile strength ratio criteria are a minimum of 0.8 or 80 %, demonstrating a mixture of asphalt that is resistant to damage caused by moisture.

Table (11): Summary of the moisture susceptibility data for the chosen asphalt mixtures.

	Designed Mixtures			
	MX1 65% CACUW	**MX2 85% CACUW**	**MX3 96% CACUW**	**MX4 104% CACUW**
S_{tm}	1525	1411	1326	1128
S_{td}	1730	1627	1593	1381
TSR	88.15	86.72	83.23	81.68
Specification Limit	Greater than or equal to 80 %.			

3. HOT MIX ASPHALT PERFORMANCE TESTS AND RESULTS

The present section will describe the procedures used to evaluate blends of asphalt in laboratories and offers the outcomes of such tests.

3.1. Samples Preparation of Hot Mix Asphalt

Cylindrical samples with a diameter of 100 mm and thickness of 63.5 mm were prepared by utilizing the Superpave Gyratory Compactor (SGC) to be used in multiple asphalt performance tests. **Table (12)** below provides a summary of the sample mass for the four aggregate mixes required to provide the proper void percentage after compacting to the required thickness.

Table (12): Mass of mixes for various types of cylindrical samples.

Mixture Type	G_{mm}	Sample Dimensions (mm)	Mass (Kg)
MX1 (65% CACUW)	2.442	D = 100, H = 63.5	1.1691
MX2 (85% CACUW)	2.440	D = 100, H = 63.5	1.1682
MX3 (96% CACUW)	2.461	D = 100, H = 63.5	1.1782
MX4 (104% CACUW)	2.465	D = 100, H = 63.5	1.1801

3.2. Static Creep Test

The static creep test determines the rutting potential of asphalt mixtures. This test was utilized in this work to estimate the parameters necessary for evaluating the viscoplastic behavior of hot mix asphalt. To determine the required parameters in ABAQUS for creating appropriate functional models (to predict the rutting phenomenon of asphalt mixtures), static creep testing was carried out with fixed compressive loads of 10, 20, and 30 psi along the diametric axis of a cylindrical specimen. For this test, cylinder-shaped testing samples of asphalt mixture are loaded with a hemispherically shaped loading ram on the Universal Testing Machine (UTM-5) for applying static axial stress. The aforementioned test is performed on cylindrical samples having a diameter of 100 mm and a thickness of 63.5 mm in unconfined conditions. The samples for testing have been produced with a Superpave gyratory compactor with an air void percentage of 4%. The sample is positioned between a pair of flat parallel loading plates and axially centered in relation to the plane of the loading plates. The displacement in the vertical direction of the samples is measured by using two linear variable differential transformers (LVDTs) positioned vertically on the top surface of the upper loading plate. Before testing begins, the sample and the loading apparatus are installed into the environmental chamber of the Universal Testing Machine, where it is given a two-hour period to become equal to the required testing temperature. This ensures that the sample has reached the required temperature for the test. Figure (4) represent a sample installed in the universal testing apparatus for the static creep investigation.

For the purpose of being able to establish good contact between the surface of the sample and loading plate, the testing procedures are set to include a ten-minute pre-loading sequence using a static axial stress of 5 kPa, which is delivered to the sample throughout the entire test, prior to performing the static creep test. The sample under examination is exposed to an axially static, haversine-shaped loading pulse as soon as the pre-loading duration finishes. The contact load provided to the sample ensures that the vertically-loaded shaft is incapable of lifting off the testing sample as well as the LVDTs respond properly.

Figure (4): Gradation of designated aggregate blends.

Figures (5) through (13) show the outcomes of static creep test for the two forms of blends of asphalt (fine as well as coarse blends) with varying aggregate gradations. Four aggregate gradations with varying percentages of coarse aggregate chosen unit weight (CACUW%) were employed.

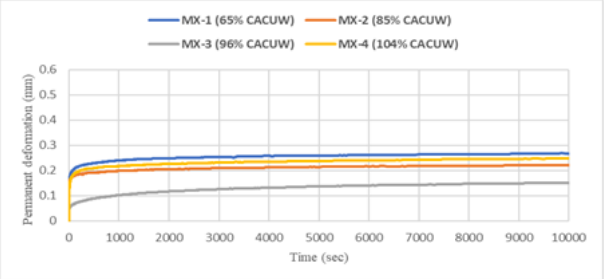

Figure (5): Creep curve for four different types of hot mix asphalt blends with various percentage of the CACUW at 10 psi stress level and 25°C temperature.

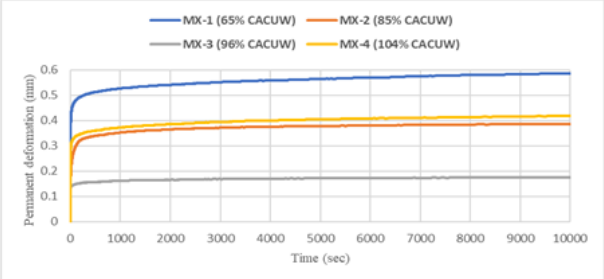

Figure (6): Creep curve for four different types of hot mix asphalt blends with various percentage of the CACUW at 20 psi stress level and 25°C temperature.

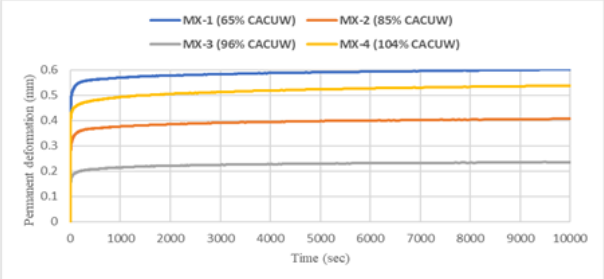

Figure (7): Creep curve for four different types of hot mix asphalt blends with various percentage of the CACUW at 30 psi stress level and 25°C temperature.

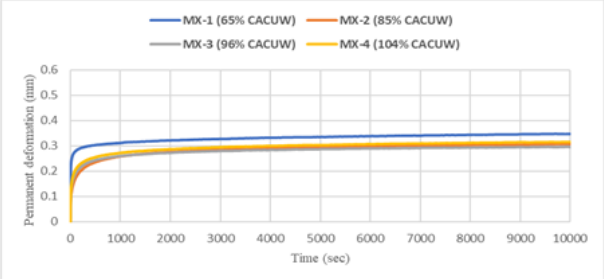

Figure (8): Creep curve for four different types of hot mix asphalt blends with various percentage of the CACUW at 10 psi stress level and 40°C temperature.

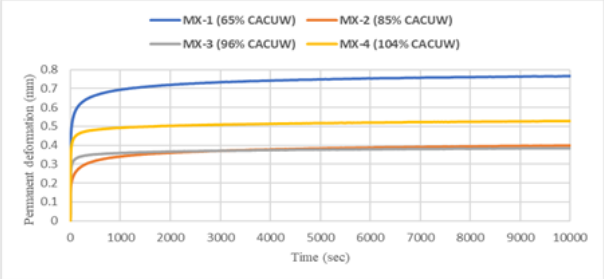

Figure (9): Creep curve for four different types of hot mix asphalt blends with various percentage of the CACUW at 20 psi stress level and 40°C temperature.

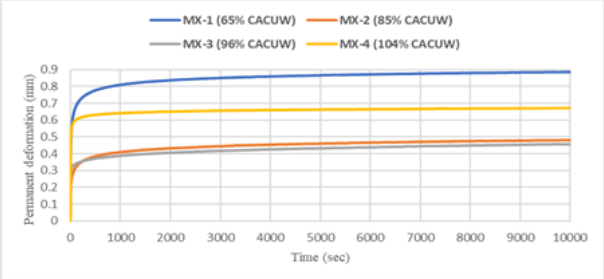

Figure (10): Creep curve for four different types of hot mix asphalt blends with various percentage of the CACUW at 30 psi stress level and 40°C temperature.

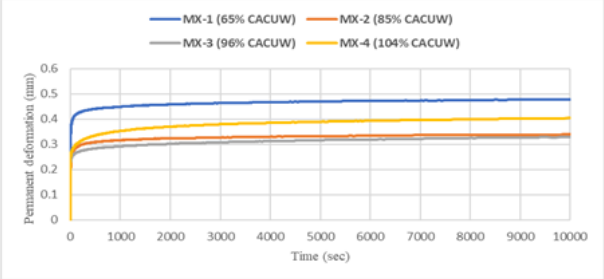

Figure (11): Creep curve for four different types of hot mix asphalt blends with various percentage of the CACUW at 10 psi stress level and 55°C temperature.

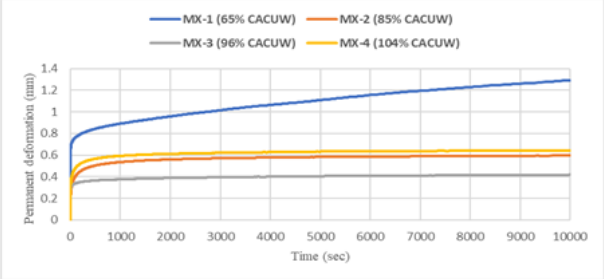

Figure (12): Creep curve for four different types of hot mix asphalt blends with various percentage of the CACUW at 20 psi stress level and 55°C temperature.

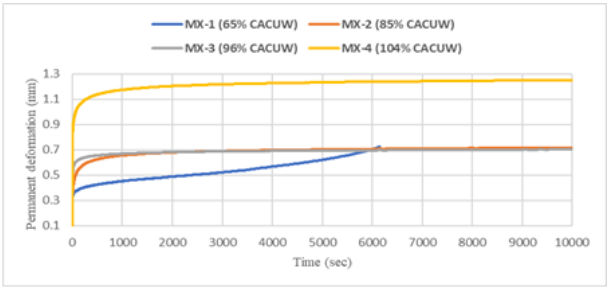

Figure (13): Creep curve for four different types of hot mix asphalt blends with various percentage of the CACUW at 30 psi stress level and 55°C temperature.

3.3. Wheel Tracking Test

An important evaluation method for figuring out how vulnerable asphalt mixtures are to rutting is the wheel tracking test, which is frequently known as the asphalt pavement rutting test. In order to characterize the rutting propensity of four differentiated mixtures of HMA prepared using the Bailey approach and Superpave procedure, the wheel tracking test was conducted at the Hami Pavement Laboratory/University of Tehran in accordance with BSI (EN 12697-22:2008) standard procedure. The aforementioned test is performed on slab testing samples having a length of 400 mm, a width of 305 mm, and a thickness of 40 mm. The samples for testing have been produced by a roller compactor in accordance with BSI (EN 12697-33:2006) with an air void percentage of 4%. Prior to testing, the produced slab samples must be allowed to cool to room temperature for a minimum of twenty-four hours. Then, they should be conditioned to the testing temperature which was 55 C^{o} and placed in the device chamber. Following the process of conditioning, the testing procedure will begin, together with the samples' deformation is going to be detected at every loading cycle employing linear variable displacement transducers (LVDT). The testing procedure is performed for a total of 10,000 cycles or until it reaches a deformation of 20 mm, whichever happens first, in accordance with the BS EN 12697-22:2003 specification.

Figure (14) present the wheel tracking outcomes from the experiment, and Table (13) demonstrate the rut depth of four various bitumen mixtures at different number of test cycles. As can be seen from the results, all bitumen mixtures perform relatively well at 10,000 cycles in terms of the rutting depth value, and there are no visible failures (d< 20mm) of all HMA samples when subjected to loading. This suggests that the HMA samples have significant resistance to rutting. The reason for this appears to be clarified through pointing out that asphalt mixtures developed with the Bailey methodology and the Superpave technique work well against rutting.

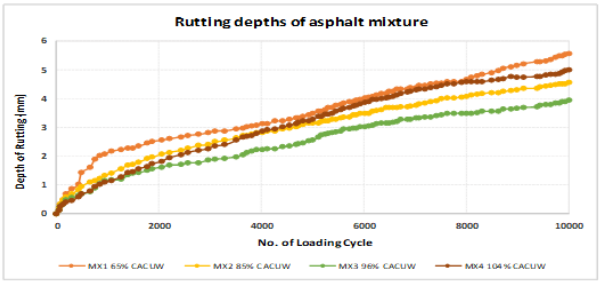

Figure (14): Wheel tracking test results for different aggregate gradation of bitumen mixtures.

Table (13): Rutting depths results of four various bitumen mixtures developed at different number of test cycles.

Mixture Type	Rutting Depth @500 cycles	Rutting Depth @2,500 cycles	Rutting Depth @5,000 cycles	Rutting Depth @7,500 cycles	Total Rutting Depth @10,000 cycles
MX1 65% CACUW	1.48	2.70	3.50	4.55	5.57
MX2 85% CACUW	0.98	2.23	3.17	3.98	4.56
MX3 96% CACUW	0.69	1.75	2.56	3.45	3.94
MX4 104% CACUW	0.70	2.11	3.27	4.46	4.98

VISCOPLASTIC FINITE ELEMENT MODELING

Viscoplastic Finite Element modeling is crucial for comprehending and forecasting how materials will behave under various loading scenarios. Because of the wide range of engineering fields in which it is applied, it is a flexible tool to use for research and real-world issues in engineering. Additionally, it is an effective tool for modeling materials that behave both viscously and plastically, such as in asphalt mixtures. To effectively estimate the performance and durability of asphalt pavements under various loads and climatic circumstances, a nonlinear time-hardening creep model must be implemented in the viscoplastic finite element modeling of hot mixed asphalts. The current finite element simulation took into account the following Equation (1) that can be found in the ABAQUS computer program to forecast rutting of flexible pavements (Abdullah, 2019).

$$\varepsilon_{vp} = A\,\sigma^{n}\,t^{m} \qquad (1)$$

Where: (ε_{vp}) is the creep strain rate; (σ) is the stress level; and (t) is the loading time.

A, n, and m, are the creep (time hardening) model parameters that correspond to the material characteristics as: (A) is the power-law multiplier; (n) is the equation stress order; and (m) is the time order. Creep parameters determined from the repeated loading and the static creep testing have been used in the finite element modeling of the wheel tracking test using ABAQUS computer software. Different slopes for different load values are depicted in Figure (15). Therefore, the average of all the weights is computed in order to get the b factor which represent the slope of the secondary zone of the static creep test. According to numerous studies, the parameter (m), which ranges from 0 to 1, is involved in Equation (1) and can be calculated using Equation (2).

$$m = b - 1 \qquad (2)$$

Finally, Table (14), displays the four mixes' parameters (b) and (m) at different temperatures for two types of tests.

Table (14): Parameters (b) and (m) determined from the slope of viscoplastic – time curves for static creep test.

Mixture	b Parameter	m Parameter	Temperature
MX-1 (65% CACUW)	0.3205	- 0.6795	55 C°
MX-2 (85% CACUW)	0.0358	- 0.9642	55 C°
MX-3 (96% CACUW)	0.0214	- 0.9786	55 C°
MX-4 (104% CACUW)	0.0463	- 0.9537	55 C°

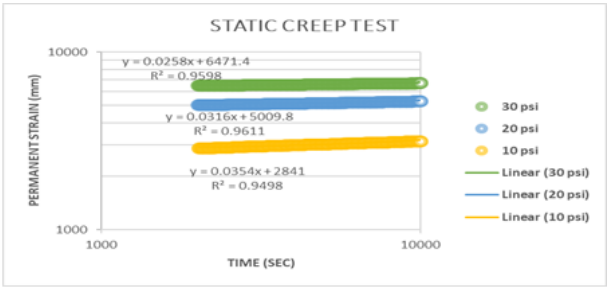

Figure (15): Viscoplastic strain relationship with time for HMA blend having 104% CACUW at various stress level and 40°C temperature.

The creep strain rate is used for representing the creep model. As a result, the strain rate must be calculated using the previously gathered strain values. An additional essential variable in assessing the rutting behavior of asphalt blends is the strain rate in relation to the time. Figure (16) shows the strain rate variation with time for all bituminous blends at various stress levels.

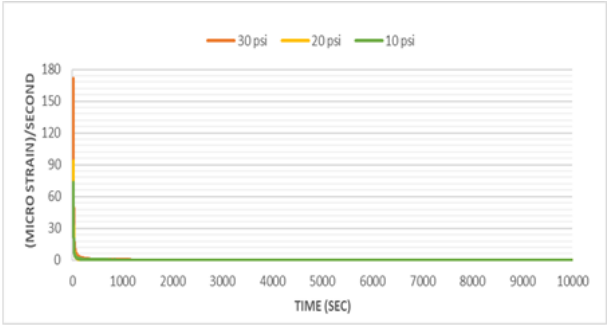

Figure (16): Strain rate curves for static creep test at various stress level and 55°C temperature.

The displayed graph demonstrates just how the strain rate exhibits an approximately the same trend. The research findings in Figure (16) indicate that when stress level rise, correspondingly increases the strain rate in the secondary zone, meaning it serves as an indicator of the viscoplastic deformation of bituminous mixes. Using Curve Expert Basic 2.23 program, nonlinear curve fitting was utilized to determine the creep parameters associated with each blend of asphalt employed in the creep model used in ABAQUS modeling. The creep model parameters are susceptible to found using the methods of multiple regression. Table (15) summarizes each of these parameters. A demonstration of fitting the strain rate curves for the HMA with 96% CACUW at 55°C in order to determine the creep parameters of the model for this blend are presented in Figure (17) and Figure (18).

Table (15): HMA creep model Parameters for static creep test and repeated loading test.

Mixture	A Parameter	n Parameter
MX-1 (65% CACUW)	$1.287307 * 10^{-6}$	1.109391
MX-2 (85% CACUW)	$3.595635 * 10^{-6}$	1.185390
MX-3 (96% CACUW)	$1.788807 * 10^{-6}$	1.152362
MX-4 (104% CACUW)	$2.056563 * 10^{-6}$	1.162251

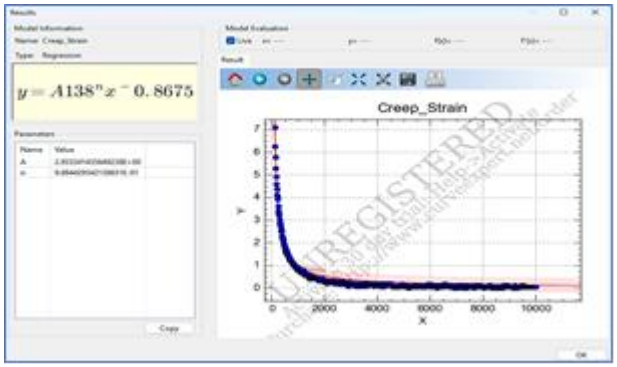

Figure (17): Fitting process of the strain rate curve of MX-3 for repeated loading test using Curve Expert Basic 2.2.3 program.

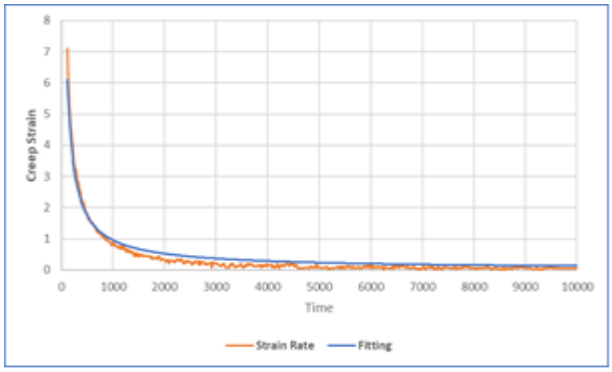

Figure (18): Fitting strain rate curve of MX-3 for repeated loading test.

FINITE ELEMENT MODELING

In the current work, Abaqus was used for generating permanent deformation models. Abaqus comprises modules that are used for the model inputs, implementation, and visualization. These modules include: part module, property module, assembly module, steps module, interaction module, load module, mesh module, job module, sketch module, and visualization module. To investigate the mechanical characteristics of the Hot Mix Asphalt (HMA), a 3-D finite element analysis of asphalt pavement reactions under repetitive loads of traffic was carried out.

The viscoplastic material properties of the asphalt blends and a repeatedly applied movement force are taken into account in this model. As shown in Figure (19), the analytical model is a hot mix asphalt slab having a dimension of 400 mm across the path of traffic, a width of 305 mm, and a thickness of 40 mm. The aforementioned measurements were selected to represent the actual wheel tracking test sample size.

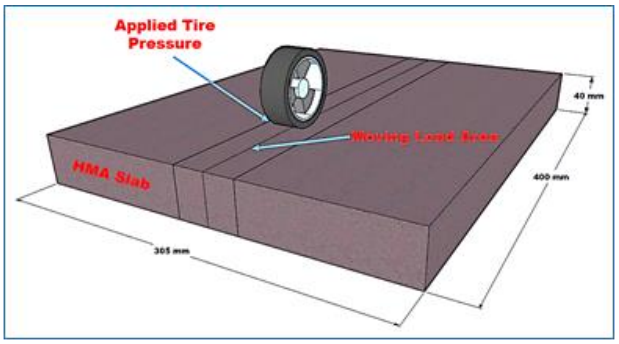

Figure (5-11): Model of a hot mix asphalt slab.

In order to minimize the computing processes and costs, the slab samples were modeled employing a quarter model, which used the symmetry boundary conditions within the symmetrical planes (Allou et al., 2015; Pérez et al., 2016; Gu et al., 2017), as demonstrated in Figure (20) below. By employing an element's formulation that creates reference to mathematical theory, the behaviour of the element can be clearly recognized.

The stiffness and mass of the element can be determined using numerical (full or reduced) integrations in the process of finite element analysis. The term "reduced integration" refers to the process of generating the element stiffness by utilizing lower-order integration. Consequently, the duration of operation will be significantly decreased particularly when dealing with three-dimensional elements. Furthermore, the strains and stresses will occur at the points that offer the best accuracy due to the decreased integration parts. Numerous numerical research solved structural issues using linear elements with reduced integration (Zeinoddini et al, 2008; Al-Thairy, 2012). So, in the process of meshing the HMA slabs for all models, the first order eight-node brick elements with reduced integration elements (C3D8R) have been used because of their high problem-solving activity. Figure (21) displays a 3-D model of finite elements mesh with the HMA slab sample surface's moving load zone that has been used for the simulation of all models.

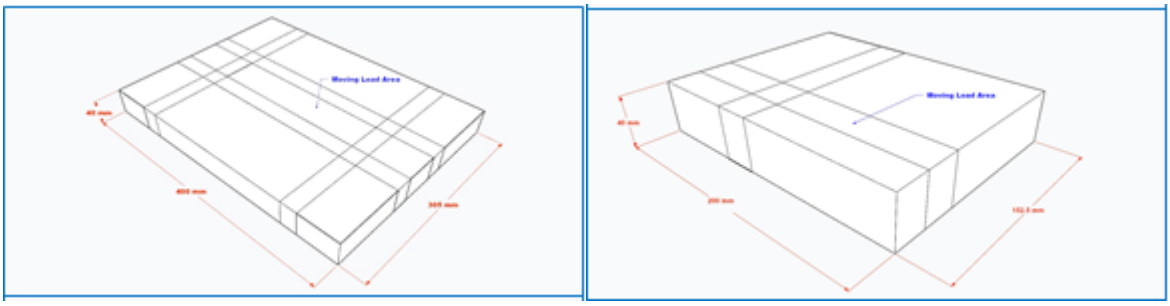

Figure (20): 3-D models for whole geometry and quarter geometry of the wheel tracking slab.

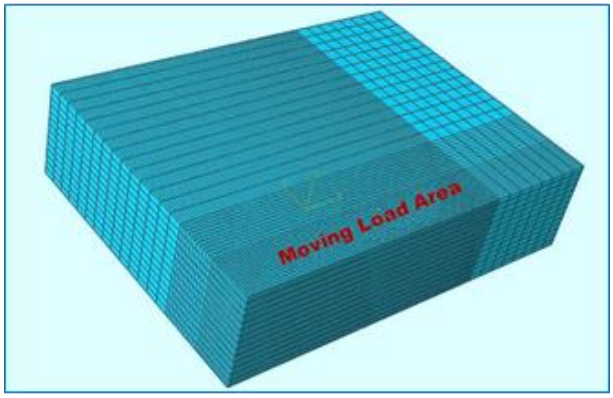

Figure (21): 3-D model for finite element meshing of pavement.

The anticipated behaviour of the pavement is significantly impacted by boundary circumstances. As a result, accurate modeling of the boundary conditions must be carried out (Zaghloul and White, 1993). In order to replicate the laboratory testing constraints, the bottom sides of the asphalt slabs were constrained in every direction to guarantee a completely fixed end which simulates what was being tested, while the top layer remained free as presented in Figure (22). Furthermore, horizontal layer edge displacements were also limited. According to what was previously stated, just one quarter of the wheel tracking slabs were actually simulated. Therefore, as symmetrical criteria, the slabs were constrained in the x-z and y-z planes

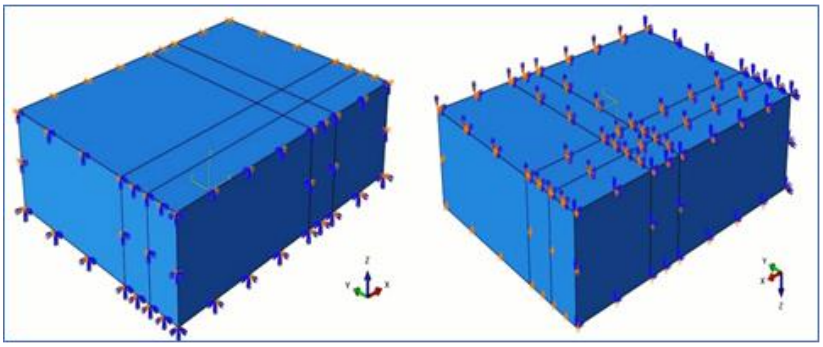

Figure (22): The boundary conditions of the wheel tracking slab (surface, sides and bottom).

The specifications of wheel tracking testing were met by applying a 700 kPa moving load as vertical uniform tire pressure on a loading area of rectangular shape having dimensions of 50 mm in width and 30 mm in length on the asphalt slab surface. The loading has been proposed to be transmitted to the pavement surface by a tire's contacting pressure. The contact pressure that occurs between the tire and the pavement is typically believed to be equally spread for purposes of simplicity (Al-Khateeb et al., 2011). A number of tiny rectangular shapes, every one approximately one-third the length of the tire footprint (10 mm) and equal in width (50 mm), were utilized for dividing the moving wheel load area. As seen in Figure (23), the wheel load covers approximately three rectangular spaces. The aforementioned aspects were utilized to compute contact pressure and time for loading (Arabani et al., 2014). During the wheel tracking test, a wheel load value of 700 N corresponded to nearly 0.5 MPa uniform loading pressure.

Figure (24) explains the wheel tracking loading sequence and loading steps employed in the finite element ABAQUS program. Figure (25) displays trapezoidal shape loading pattern that reflected the amplitude of the loading waveform for each loaded area. At time t_0, the load intensity is zero, which represents the beginning of the loading cycle. Following time t_0, the load increases gradually from zero until time t_1, when it reaches its optimum amount. The load intensity stays unchanged from time t_1 to time t_2, following that it decreases gradually from its highest value to zero at time t_3 (i.e., it follows a trapezoidal ramp) before going to the following elements set and carrying out this loading procedure repeatedly (Saleh and Ghorban, 2017).

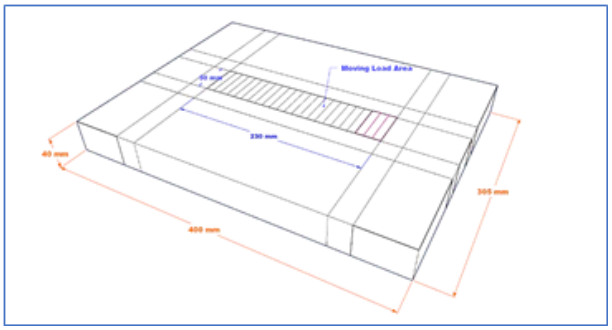

Figure (23): Moving wheel load area.

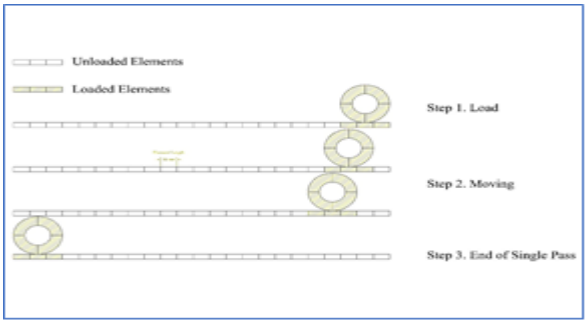

Figure (24): Schematic of moving load.

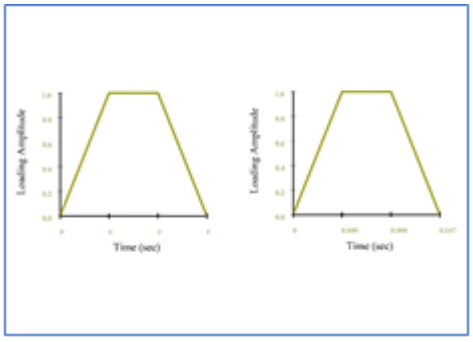

Figure (25): Schematic of loading amplitude (trapezoidal waveform).

While various finite element programs provide multiple increment types, which can be exponential or possibly sinusoidal for cyclic loading, the linear increase during the loading duration is the standard. In the present study, loading was increased linearly from zero to the predefined maximum (Carvalho, 2012). The duration of loading is a relationship between tire footprint length and the wheel velocity. Therefore, the duration of loading for the wheel footprint of 30 mm in length will be 0.147 s, which determined by dividing the wheel

footprint by the wheel velocity. According to the loading waveform mentioned before, the duration is divided into three equal zones as displayed in Figure (25). The first zone is loading zone where there is gradual increase in loading intensity from zero to maximum loading and represented by the period between t_0 to t_1. Then the steady loading zone where the loading intensity are constant at maximum loading which is represented by period between t_1 to t_2. Finally, the unloaded zone where there is gradual decrease in loading intensity from maximum loading to zero and represented by the period between t_2 to t_3. The wheel pass time can be determined by dividing the moving loading path over the wheel velocity, which is approximately equals 1.132 seconds.

The cumulative time for loading is calculated by multiplying the loading time by the overall amount of loading cycles. Since it takes 2.264 seconds to load a complete wheel cycle, the total time needed to load for the whole examination, which consists of 10,000 cycles, is 22640 seconds. The process described above takes a lot of time, but it represents a cyclical moving wheel much more accurately. The anticipated model's load application technique was completely compliant with the wheel tracking test requirements (Bakhshi and Arabani, 2018).

The module will need to be examined once all of the activities related to the creation of the model have been performed. In ABAQUS, the activities associated with solving a FEA model can be built and handled in the Job Module. Users can handle the results files and build, execute, and track analysis jobs with it. Particularly important for handling various simulation jobs is the Job Module, which acts as a link between the pre-processing stage (where the model is generated) and the post-processing stage (where the outcomes are examined). The Visualization Module represents the place where it is possible to examine, comprehend and display the output data after the analysis task is finished and the outcomes become ready. ABAQUS offers a full range of options for analyzing results, such as contours charting, data graphing, and graphical representations. The permanent deformation shape of bituminous blend with 104% CACUW after 10000 cycles, is illustrated in Figure (26).

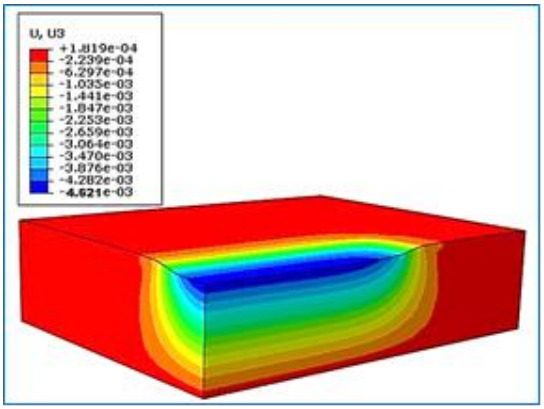

Figure (26): Permanent deformation shape of MX-4 at 55 °C under repeated loading test.

A validation procedure was conducted by contrasting the resulting data from finite element modeling with the laboratory findings with the objective to confirm the finite element model. To compare the rutting results predicted by the model with the real outcomes of rutting (permanent deformation), an identical set of tests were previously carried out utilizing wheel tracking testing. The purpose of using this method is to ensure that the model is applicable and accurate in predicting the response of the asphalt blends.

Throughout the process of testing, the asphalt slab samples were tested under 700 kPa of repeated moving tire pressure. The overall path of the tire across the slab is 230 mm. The asphalt slab samples were made using four different kinds of HMA mixes. The HMA mixtures were MX-1 with 65% CACUW, MX-2 with 85% CACUW, MX-3 with 96% CACUW, and MX-4 with 104% CACUW. Each slab was then subjected to the wheel track test at 55 °C. The purpose of the wheel tracking experiments was to determine the depth of ruts on the asphalt slab surface beneath and along the path taken by the wheel at 10,000 cycles.

To achieve the main objective of the current study, four models were developed to predict the rutting of asphalt mixtures. The simulation was validated by comparing the actual rutting from the wheel tracking testing at varying numbers of loading cycles with the rutting rates of asphalt blends forecasted depending on the viscoplastic model.

Since the model must employ a repeated moving surface load to represent the moving wheel load, only a minor adjustment was necessary in order to represent the repeated moving load. The temperature, boundary conditions, wheel speed, overall amount of load cycles, loading and unloading times, as well as additional modeling parameters, however, were unchanged. It was discovered that these asphalt surfaces could have been sufficiently deformed by the overall amount of load cycles submitted to the asphalt slab surface.

The results show varying differences between the measured and predicted rutting. By analyzing the results in Figures (27) to (30), we notice that the percentage of variation between the permanent deformation resulting from the laboratory test and the permanent deformation predicted using the results of the static creep test is very small. The aforementioned figures compare the rutting predicted by the viscoplastic model for the static creep with the rutting observed on the HMA layer surface under the center of the moving wheel path. It is evident from the evaluation of overall strain that the laboratory response and the FEM-simulated HMA response are nearly close. The slight variations regarding actual and anticipated rutting result from the model's assumption that the material characteristics are homogeneous and uniform, while the blends really contain various aggregate interlocks along with certain voids.

Additionally, in practice, both the temperature and viscosity of the blends are incapable of being spread uniformly throughout the blend, which makes modeling extremely challenging due to the complexity of varying the temperature and viscosity for every blend component (Shanbara et al., 2018). On the other hand, the aforementioned variations have no impact on the validation of the finite element model. The variations among the Laboratory rut depth and predicted rutting depths are presented in Table (16).

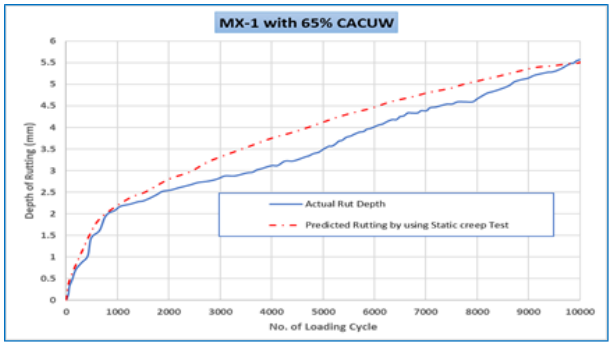

Figure (27): Actual and predicted rutting depth for MX-1.

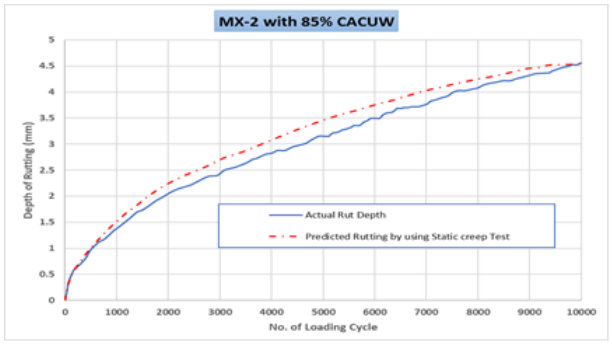

Figure (28): Actual and predicted rutting depth for MX-2.

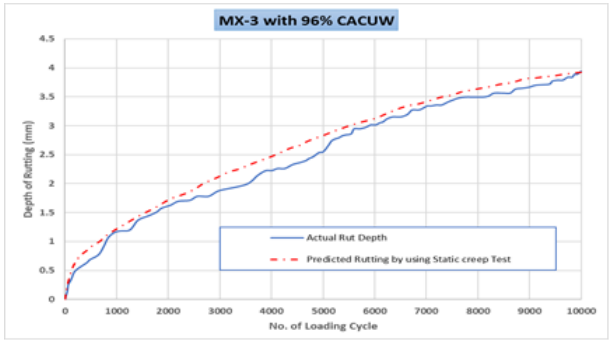

Figure (29): Actual and predicted rutting depth for MX-3.

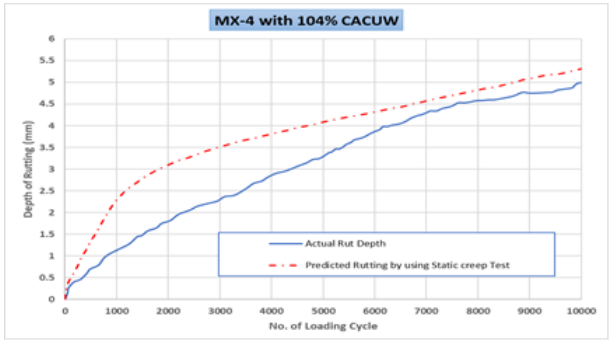

Figure (30): Actual and predicted rutting depth for MX-4.

Table (16): Variations between the laboratory and predicted rutting depths at the end of 10,000 cycles.

Mixture Type	Laboratory rut depth (mm)	Predicted rut depth (mm)	Variation
MX-1 (65% CACUW)	5.57	5.51	% 1.1
MX-2 (85% CACUW)	4.56	4.55	% 0.2
MX-3 (96% CACUW)	3.94	3.92	% 0.5
MX-4 (104% CACUW)	4.98	5.31	6.6 %

CONCLUSION

The present research forecasted the rutting behavior of the hot mix asphalt in the wheel tracking test using the 2D and 3D finite-element methods. The accelerated creep phase (plastic deformation) of the HMA blend was modeled using the ABAQUS software. The CPE4R and C3D8R elements for 2D and 3D models, consequently, have been employed to assess the WTT outcomes. The existing creep power law model from the ABAQUS library was utilized in the finite element modeling, then the findings of the static creep test were analyzed to determine the creep parameters of the proposed model. The subsequent conclusions were drawn from the outcomes of 2D and 3D modelling:

1. The results of this study show that the anticipated and actual rutting depths match very closely. As a result, the creep model is frequently used in finite element analysis when predicting the rutting characteristics of asphalt blends.

2. It provides an accurate estimation of the rutting depth and is therefore seen to serve as a helpful instrument for analyzing the rutting of hot asphalt mixtures.

ACKNOWLEDGEMENTS

This article is a part of Ph.D. dissertation in Civil Engineering at Al-Nahrain University.

REFERENCES

[1] Ali, Y., Irfan, M., Ahmed, S., & Ahmed, S., 2017. Empirical correlation of permanent deformation tests for evaluating the rutting response of conventional asphaltic concrete mixtures. Journal of Materials in Civil Engineering, 29(8), 04017059.
[2] Irfan, M, Y Ali, S Iqbal, S Ahmed, and I Hafeez., 2018. Rutting evaluation of asphalt mixtures using static, dynamic, and repeated creep load tests, Arabian Journal for Science and Engineering, 43: 5143-55.
[3] Vavrik, W. R., Pine, W. J., & Carpenter, S. H., 2002. Aggregate blending for asphalt mix design: Bailey method. Transportation Research Record, 1789(1), 146-153.
[4] Aodah, Haider Habeeb., 2013. PERFORMANCE PREDICTION MODEL FOR BITUMINOUS MIXES, PhD thesis, Indian institute of technology roorkee.
[5] Bathe, K., 1995. Finite Element Procedures.
[6] Robert D. Cook, Malkus, Plesha, Witt., 2002. Concepts and Applications of Finite Element Analysis, 4TH ED. University of Wisconsin – Madison. Jhon Wiley and Sons, INC.
[7] Bakhshi, B. and Arabani, M., 2018. Numerical evaluation of rutting in rubberized asphalt mixture using finite element modeling based on experimental viscoelastic properties. Journal of Materials in Civil Engineering, 30(6), p.04018088.
[8] Ebrahimi, M.G., 2015. Investigation of viscoelastic behaviour and permanent deformation modelling for New Zealand hot mix asphalts (Doctoral dissertation, University of Canterbury).
[9] Holanda, Á.S.D., Parente Junior, E., Araújo, T.D.P.D., Melo, L.T.B.D., Evangelista Junior, F. and Soares, J.B., 2006. Finite element modeling of flexible pavements. Iberian Latin American Congress on Computational Methods in Engineering.
[10] Carvalho, R.L., 2012. Prediction of permanent deformation in asphalt concrete (Doctoral dissertation, University of Maryland).
[11] Institute, A., 2014. Asphalt Mix Design Methods. Manual Series No. 2, (MS-2).
[12] Abdullah, G.M., 2019. 3D finite element modeling to predict the foamed sulfur asphalt marl soil mixes rutting behavior. Ain Shams Engineering Journal, 10(4), pp.661-668.
[13] Allou, F., Takarli, M., Dubois, F., Petit, C. and Absi, J., 2015. Numerical finite element formulation of the 3D linear viscoelastic material model: Complex Poisson's ratio of bituminous mixtures. Archives of Civil and Mechanical Engineering, 15 (4), 1138-1148.
[14] Gu, F., Luo, X., Luo, R., Hajj, E.Y. and Lytton, R.L., 2017. A mechanistic-empirical approach to quantify the influence of geogrid on the performance of flexible pavement structures. Transportation Geotechnics, 13, 69-80.
[15] Pérez, I., Medina, L. and del Val, M.A., 2016. Nonlinear elasto–plastic performance prediction of materials stabilized with bitumen emulsion in rural road pavements. Advances in Engineering Software, 91, 69-79.
[16] Zeinoddini, M., Harding, J.E. and Parke, G.A.R., 2008. Axially pre-loaded steel tubes subjected to lateral impacts (a numerical simulation). International Journal of Impact Engineering, 35 (11), 1267-1279.
[17] Al-Thairy, H., 2012. Behaviour and Design of Steel Column Subjected to Vehicle Impact. PhD Thesis, University of Manchester.
[18] Zaghloul, S.M. and White, T., 1993. Use of a three-dimensional, dynamic finite element program for analysis of flexible pavement. Transportation research record, (1388).
[19] Al-Khateeb, L.A., Saoud, A. and Al-Msouti, M.F., 2011. Rutting prediction flexible pavements using finite element modeling. Jordan Journal of Civil Engineering, 159(2980), pp.1-18.
[20] Arabani, M., Jamshidi, R. and Sadeghnejad, M., 2014. Using of 2D finite element modeling to predict the glasphalt mixture rutting behavior. Construction and Building Materials, 68, 183-191.
[21] Saleh, M. and Ghorban Ebrahimi, M., 2017. Finite Element Modeling of Permanent Deformation in the Loaded Wheel Tracker Test. Transportation Research Record, 2641(1), pp.94-102.